Two Superhelix Density-Dependent DNA Transitions Detected by Changes in DNA Adsorption/Desorption Behavior†

Miroslav Fojta,‡ Richard P. Bowater,§ Veronika Staňková,‡ Luděk Havran,‡ David M. J. Lilley,|| and Emil Paleček*,‡

Institute of Biophysics, Academy of Sciences of the Czech Republic, 612 65 Brno, Czech Republic, Imperial Cancer Research Fund, Clare Hall Laboratories, South Mimms, Hetfordshire ENG 3CD, United Kingdom, and CRC Nucleic Acid Structure Research Group, Department of Biochemistry, University of Dundee, Dundee DD1 4HN, United Kingdom

Received December 2, 1997

ABSTRACT: The adsorption behavior of covalently closed circular plasmid DNA at the mercury/water interface was studied by means of AC impedance measurements. The dependence of the differential capacitance (C) of the electrode double layer on the potential (E) was measured in the presence of adsorbed DNA. It was found that the $C-E$ curves of supercoiled DNA at native and highly negative superhelix densities (σ), relaxed covalently closed circular DNA, and nicked DNA differed from each other. A detailed study of topoisomer distributions ranging from $-\sigma$ of 0 to 0.11 revealed two supercoiling-dependent transitions, at about $-\sigma = 0.04$ (transition TI) and 0.07 (transition TII). Transition TI was detected by measuring the height of the adsorption/desorption peak 1 (at about −1.2 V against the saturated calomel electrode) and the decrease of capacitance (ΔC) at −0.35 V. This transition may be due to a sudden change in the ability of the DNA to respond to the alternating voltage, probably caused by changes in the DNA tertiary and/or secondary structure. Transition TII was detected by measuring peak 3* (at about −1.3 V), which was absent in topoisomers with $-\sigma$ less than 0.05. This transition is due to changes in the DNA adsorption/desorption behavior related to increased accessibility of bases at elevated negative superhelix density. Opening of the duplex at highly negative superhelix density was also detected by the single-strand selective probe of DNA structure, osmium tetroxide, 2,2′-bipyridine. Our results suggest that electrochemical techniques provide sensitive experimental analysis of changes in DNA structure.

Negative supercoiling can promote changes in both global and local structure in DNA. Any structure that brings about a negative change in twist, equivalent to an underwinding of the helix, will be stabilized by negative supercoiling. This includes many sequence-dependent variants of DNA structure, including local helix opening and the formation of cruciform structures, triplex H-DNA, or left-handed Z-DNA (*1*).

Unusual DNA structures produce changes in local twist and the overall shape of the supercoiled DNA molecule because of the compensatory changes in writhe, and this may often be detected by two-dimensional gel electrophoresis (*2*). The observed transitions can usually be fitted to a statistical mechanical model of the structural change and its interaction with the overall topology of the molecule. Frequently the perturbed DNA structure leads to the exposure of particular bases in a way that is distinct from regular B-DNA. As an example, this may result in an enhanced reactivity toward a chemical reagent (*1*, *3*).

Experimental methods suitable for studies of supercoiled DNA species are rather limited in general. No crystals have been obtained to date of supercoiled DNA circles, and the molecules are too large to be studied by NMR. Electron microscopy and cryoelectron microscopy have been very important in the study of the global shapes of supercoiled DNA (*4*, *5*). Circular dichroism, Raman spectroscopy, time-resolved fluorescence anisotropy measurements of intercalated ethidium, and dynamic light scattering have recently been applied to the study of supercoiled DNA (reviewed in ref *6*). In general the conformational problem is sufficiently complex to require a combination of experimental approaches with theoretical analysis.

Adsorption of biomacromolecules at surfaces is of great importance in nature and in contemporal biotechnologies. The literature on the adsorption of proteins is quite extensive (reviewed in refs *7*−*9*). Redox processes at electrodes have been mainly used to report about the changes in DNA structure and properties (reviewed in refs *10*−*12*), but adsorption/desorption properties of DNA have been studied to a lesser extent (refs *10* and *13* and references cited therein). AC impedance measurements represent one of the methods suitable for the analysis of biomacromolecules (*9*).

Electrochemical methods provided an early indication of premelting and structural polymorphism of DNA (*14*). Mercury electrodes have been shown to be highly sensitive to conformational changes in DNA molecules (*14*) as well

† This work was supported by a grant of the Grant Agency of the Czech Republic (204/97/K084 and 204/96/1680) to E.P., by financial support of the Cancer Research Campaign to D.M.J.L., and by a grant of the Royal Society for a visit to the Czech Republic to R.P.B.

* To whom correspondence should be addressed. Fax: ++4205 4121 1293; e-mail: palecek@ibp.cz.

‡ Academy of Sciences of the Czech Republic.

§ Clare Hall Laboratories.

|| University of Dundee.

S0006-2960(97)02955-3 CCC: $15.00
Published on Web 03/18/1998

as minor DNA damage (reviewed in refs *10* and *12*). In the past decade, transfer stripping techniques, in which DNA can be immobilized at a mercury electrode from 4 to 5 μL drops of solution, make it possible to study submicrogram DNA samples, providing electrochemical responses not significantly different from those obtained in conventional voltammetric techniques where the amounts of material required are 2−3 orders of magnitude higher. It is therefore feasible to use electrochemical methods for studies of supercoiled plasmid DNA samples, including topoisomer distributions of selected mean linking difference.

In this paper, we measure the alternating current (AC)[1] impedance of the electrode double layer in the presence of DNA adsorbed at the atomically flat surface of the mercury electrode over a wide potential range. To minimize the volume of a DNA solution, we use the adsorptive transfer technique, which is based on the adsorption of DNA at the electrode followed by AC impedance measurement with the electrode immersed in a blank background electrolyte. Using this technique, we show that the adsorption/desorption behavior of covalently closed circular DNA is influenced by the DNA superhelix density. Studies of topoisomer distributions show two superhelix density-dependent transitions at midpoints of $-\sigma$ about 0.04 and 0.07.

EXPERIMENTAL PROCEDURES

Preparation of DNA Samples. Plasmid DNAs pAT153 (3.6 kb) (*15*), pBR322 (4.4 kb), pUC19 (2.7 kb) (*16*), and pColIRΔXba (3.7 kb) (*17*) were isolated as described (*18*).

Preparation of plasmid topoisomer distributions of defined mean superhelix density [specific linking difference, $\sigma = (Lk - Lk_0)/Lk_0$, where the meanings of Lk and Lk_0 are the linking number of the given DNA topoisomer and the linking number of relaxed DNA molecule of the same primary structure, respectively]. Distributions of topoisomers were obtained by incubating native supercoiled plasmid DNA with wheat germ topoisomerase I (Promega) in the presence of various concentrations of ethidium bromide (*2*, *19*). After phenol/chloroform extraction of the protein, the DNA was recovered by ethanol precipitation, dissolved in 10 mM Tris-HCl, pH 7.5, and 0.1 mM EDTA (TE buffer). The range of linking numbers within each distribution was determined by comparison of the samples on the agarose gels containing various concentrations of choloroquine (at least four different concentrations were used for each of the reactions).

Preparation of Open Circular, Linear, and Denatured DNA. Linear plasmid DNA species were prepared by *Eco*RI or *Bam*HI (Fermentas) cleavage of supercoiled DNA (*16*). DNA was deproteinized by extraction with a mixture of phenol, chloroform, and isoamyl alcohol (25:24:1), twice extracted with chloroform and precipitated with ethanol (*16*) and dissolved in TE buffer. To obtain open circular DNA, supercoiled DNA (100 μg mL^{-1}) was γ-irradiated using a Chisostat (Chirana, Brno) ^{60}Co source in Eppendorf tubes containing 20 μL of the DNA solution in 0.2 M NaCl/10 mM TE buffer, pH 7.4 (NT buffer), at room temperature. Denatured DNA was prepared by heating of linear DNA in TE buffer for 5 min at 96 °C followed by rapid cooling on ice. Concentrations of the stock DNA solutions were determined by measuring the absorbance at 260 nm. All DNA samples were stored at −20 °C in TE buffer.

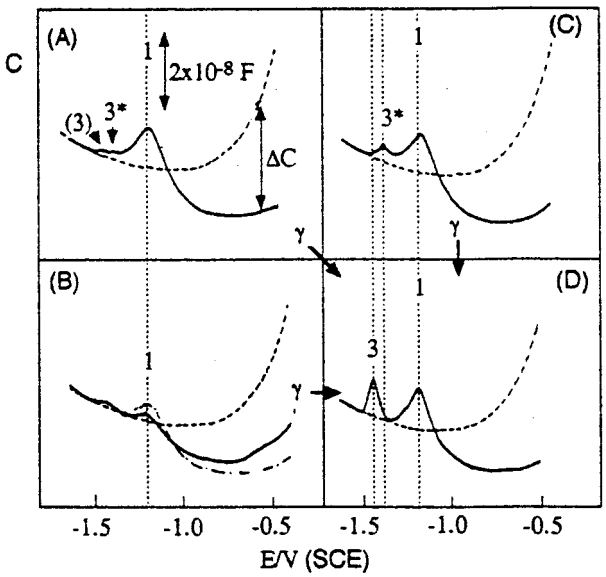

FIGURE 1: Sections of $C-E$ curves of a hanging mercury drop electrode modified with pUC19 DNA: A, supercoiled DNA at native superhelix density; B, topoisomerase I-relaxed DNA; C, highly supercoiled DNA ($-\sigma \geq 0.11$); D, open circular DNA. DNA concentration was 100 μg mL^{-1}, adsorption time $t_A = 120$ s; in B, (−·−), 250 μg mL^{-1}, $t_A = 180$ s; (- - -), background electrolyte. The response of open circular DNA prepared from covalently closed circular DNA by γ-irradiation (arrows marked "γ") was not influenced by the superhelix density of the original covalently closed circular DNA. In panel A, the meaning of the capacitance decrease (ΔC) is displayed. DNA was adsorbed at the electrode from a drop (4 μL) of solution containing 0.2 M NaCl and 0.01 M Tris-HCl buffer, pH 7.4 (NT buffer), at room temperature. DNA-modified electrodes were then washed in water and in background electrolyte solution and placed into a cell containing blank background electrolyte (0.3 M NaCl, 0.05 M sodium phosphate, pH 8.5). Prior to the measurements, argon was bubbled through the electrolyte solution for 60 s.

Electrochemical Measurements. Alternating current (AC) impedance (Z) measurements can be utilized for the detection as well as for quantitation of adsorption of surface active substances at the electrode surface (refs *9* and *20* and references cited therein). Adsorption of DNA at the electrode results in a decrease of the capacity C (ΔC) of the electrode in a wide range of potentials below the value C_0 (Figure 1) yielded by the bare electrode (immersed into the background electrolyte). The decrease $\Delta C = C_0 - C$ is related to the adsorbed amount of the given nucleic acid.

The measurements were performed with a EG&G PAR 174A polarographic analyzer connected to 174/50 AC polarographic interface, 5208 two phase lock-in amplifier, and a Philips PM 8134 X_t Y_1 Y_2 recorder. The following parameters were chosen: frequency 230 Hz, peak-to-peak amplitude 10 mV, scan rate 20 mV s^{-1}, initial potential −0.2 V. In measurements using the dropping mercury electrode, the lifetime of the static mercury drop electrode (SMDE) was 10 s and the scan rate was 1 mV s^{-1}. In some cases, AC Z measurements were performed using an Autolab (EcoChemie, Utrecht, The Netherlands) at the following settings: amplitude 10 mV, equilibration time 1 s, integration time 0.2 s, potential step 37 mV, frequency 297 Hz.

[1] Abbreviations: C, capacitance; E, potential; AC, alternating current; Z, impedance; I, current; AdTS, adsorptive transfer stripping; CV, cyclic voltammetry; DPV, differential pulse voltammetry; p, peak height; Os,-bipy, osmium tetroxide 2,2′-bipyridine; σ, superhelix density.

Measurements were performed in 0.3 M NaCl/0.05 M sodium phosphate, pH 8.5 (NP buffer), or in 0.3 M NaCl/0.03 M sodium bicarbonate, pH 9.5 (NC buffer). Alkaline pH was used to prevent the faradaic (redox) processes requiring protonation of bases and to obtain well-developed capacitive responses. No significant changes in the DNA AC *Z* responses were observed in the pH range between 8.0 and 10.0 (not shown).

Cyclic voltammetry (CV) was performed with a PAR 362 scanning potentiostat (scan rate 0.2 V s^{-1}, initial potential −0.1 V, switching potential −1.85 V) using 0.3 M ammonium formate/0.05 sodium phosphate, pH 6.9 (AFP), as background electrolyte. Presence of ammonium ions in the background electrolyte is important for reduction of bases if the measurements are performed at pH values close to neutral.

Differential pulse voltammetry (DPV) was performed with an Autolab (EcoChemie, Utrecht, The Netherlands) (scan rate 20 mV s^{-1}, pulse amplitude 50 mV, modulation time 0.04 s, time interval 0.4 s, potential step 8 mV) in AFP.

UV spectra were measured with a Hewlett-Packard 8452A diode array spectrophotometer in a 1 cm quartz cuvette.

Preparation of DNA-Modified Electrodes. Electrochemical measurements were mostly performed using adsorptive transfer stripping (AdTS) with DNA-modified electrodes (*12*, *21*, *22*). DNA was adsorbed at the electrode surface from 4 μL drops of solution containing 0.2 M NaCl and 10 mM Tris-HCl, pH 7.4 (NT buffer). The DNA-modified electrode was washed twice by distilled water and by background electrolyte solution and transferred into deaerated blank background electrolyte, which was then perfused with argon for 90 s. The initial potential (E_i) was applied at the electrode for 15 s (quiescent period) prior to the voltage scan. A Metrohm 647 VA-Stand electrode in HMDE or SMDE mode controlled by Metrohm 646 VA-Processor was used. All measurements were performed with saturated calomel reference electrode (SCE) and a platinum wire counter electrode.

We have shown (*13*, *22*, *23*) that the DNA responses obtained by various methods including AC impedance measurements in the conventional way (with the electrode dipped in the DNA solution) do not substantially differ from those obtained with the DNA-modified electrode immersed in the background electrolyte (not containing any DNA). A good agreement between the AC impedance measurements obtained in the two above ways supports the notion (*10*, *13*) that the adsorption/desorption DNA peaks cannot merely correspond to the AC impedance peaks, usual in low molecular mass compounds, which reflect a rapid exchange between the adsorbed and solution species (*24*, *25*). In nucleic acids (and other polymers), these peaks are usually due to adsorption/desorption (or reorientation) of segments of the molecule (e.g., parts of DNA strands extending in solution may exchange rapidly with the trains of adsorbed DNA segment). In principle, the nucleic acid molecule may remain anchored at the surface even if its major part extends to the solution; such a behavior has been recently demonstrated with DNA and peptide nucleic acid decamers (*13*).

Chemical Modification. The DNA samples (10 μg mL^{-1}) were treated with 2 mM osmium tetroxide/2 mM 2,2′-bipyridine (Os,bipy) in NT buffer for 30 min at room temperature. The reaction was stopped by two extractions with chloroform followed by ethanol precipitation. The DNA was pelleted by centrifugation, rinsed twice in 80% ethanol, and dissolved in 10 mM TE buffer. Single-stranded pAT153 (denatured linDNA) modified with 4 mM Os,bipy at 37 °C for 20 h was used for calibration.

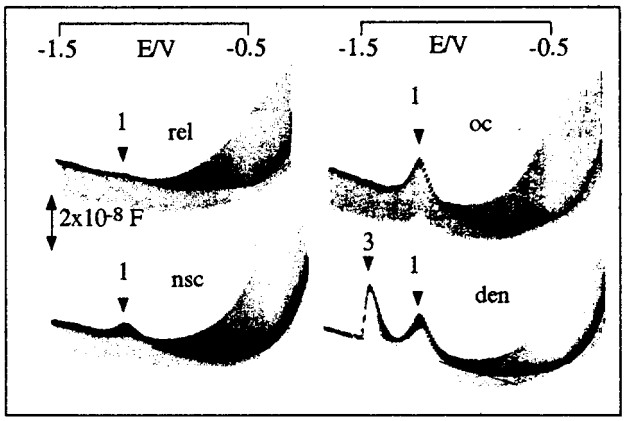

FIGURE 2: *C*−*E* curves obtained using a stationary mercury dropping electrode produced by various forms of pUC19 DNA (indicated in the figure) measured in 0.3 M NaCl 0.03 M $NaHCO_3$, pH 9.5. Scan rate 1 mV s^{-1}, drop lifetime 10 s. DNA concentration 200 μg mL^{-1}. Measurements were performed on 80−100 μL of solution on air. In contrast to the other AC impedance measurements, in this experiment the mercury electrode was immersed directly in the DNA solution during the measurements. Panels rel, relaxed DNA; oc, open circular DNA; nsc, native supercoiled DNA; den, denatured linear DNA.

Voltammetric Determination of the DNA−*Os,bipy Adduct*. Prior to the AdTS DPV measurements, the samples were nicked with DNase I (0.1 U mL^{-1} in 40 mM Tris-HCl, pH 7.4, 6 mM $MgCl_2$, 2 mM $CaCl_2$, 10 min, 37 °C; the conditions were pretested) and thermally denatured in order to remove the possible influence of DNA structure on its voltammetric response. Ratios of the areas of the adduct-specific DPV signal at −1.09 V (see Results) and CV peak G yielded by the same sample [which is insensitive to the DNA modification with Os,bipy due to a negligible reactivity of guanine residues toward the probe (*26*)] were calculated to eliminate the influence of uncontrolled changes in DNA concentration during ethanol precipitation. [In an analogous way, the influence of DNA surface concentration on the height AC *Z* peak 1 was eliminated using the capacity decrease, ΔC (see Figure 2 and Results).] In this way, a reasonable agreement between the results at DNA concentrations below and above 20 μg mL^{-1} was obtained.

S1 Nuclease Cleavage. The DNA samples were treated with S1 nuclease (Pharmacia) in 60 mM sodium acetate (pH 4.6), 50 mM NaCl, 1 mM $ZnCl_2$, and 50% glycerol, at 37 °C for 30 min. The reaction was terminated by the addition of 0.05 M EDTA, and the samples were loaded on the agarose gel.

Gel Electrophoresis. Samples of DNA were electrophoresed in 1% agarose gels containing 40 mM Tris acetate (pH 7.8)/1 mM EDTA using a voltage gradient of 3−4 V cm^{-1}. The gels were stained with 1 μg mL^{-1} ethidium bromide and photographed under illumination by UV light.

Immuno Dot Blotting Analysis. Modified DNA was applied to a nitrocellulose membrane (Schleicher and Schuell) in 2-fold dilution series. After the membrane was dry, it was incubated with 140 mM NaCl, 3 mM KCl, 80 mM Na_2HPO_4, and 18 mM KH_2PO_4 (PBS) containing 5% dried milk

(MPBS) for 1 h at 37 °C to block the nonspecific binding. Then the primary monoclonal antibody OsBP95-1 (*27*) was added into the MPBS in the final concentration of 30 μg mL^{-1} and incubated for another hour at 37 °C, followed by washing with PBS containing 0.05% Tween (PBST) four times. Then the membrane was incubated with the secondary alkaline phosphatase-conjugated goat anti-mouse IgG (Fc-specific) (Sigma) for 1 h at 37 °C, followed by washing with PBST four times. This second antibody was diluted 1000 times into the MPBS. The membrane was transferred into carbonate buffer (100 mM $NaHCO_3$, 1 mM $MgCl_2$, pH 9.8), and 0.13 M 5-bromo-4-chloro-3-indolyl phosphate (BCIP) and 0.06 M nitrobluetatrazolium chloride (NBT) were added to develop the color signal.

RESULTS

Adsorption/Desorption Behavior of Relaxed and Supercoiled DNAs. Electrochemical measurements can provide information about the interaction of DNA with electrically charged interfaces, including the exposure of bases upon interaction with an electrode surface. Using adsorptive transfer stripping cyclic voltammetry, quantitative differences in the redox signals of supercoiled and linearized DNA were observed (*28*). AC impedance measurements represent a useful method for studies of DNA adsorption that is not perturbed by chemical reactions that may accompany the DNA redox processes at electrodes. Earlier it was shown that DNA adsorption is structure-dependent (reviewed in ref *10*). Recently, we have shown that AC impedance responses of supercoiled plasmid DNA differ qualitatively from that of chromosomal DNA and open circular and linear plasmid DNA (*29*). Under standard conditions, the latter DNA species produce peak 3 at about −1.43 V (specific for single-stranded DNA) as a result of helix unwinding occurring on the surface during the potential scan. With covalently closed circular (ccc) DNA, the unwinding is topologically limited, and thus this peak is absent (*29*).

Here we measured the dependence of the capacitance (C) on the potential (E) in the range of −0.5 to −1.65 V ($C-E$ curves) for the plasmid pUC19, using the hanging mercury drop electrode (HMDE). The DNA was studied at full surface coverage in supercoiled forms at native superhelix density (σ) (Figure 1A) and at highly negative superhelix density (Figure 1C), as well as with topoisomerase I-relaxed DNA (Figure 1B) and nicked circular (irradiated by γ-radiation) DNA (Figure 1D). DNA samples (100 μg of DNA/mL) were adsorbed at the electrode in 10 mM Tris-HCl/0.2 M NaCl, pH 7.4, and measured in 0.3 M NaCl/50 mM sodium phosphate, pH 8.5. All DNA samples exhibited a decrease of capacitance (ΔC) in the potential range −0.5 and −1.0 V, suggesting that DNA is adsorbed at the electrode surface under these conditions. The observed potential-dependent changes in ΔC are in qualitative agreement with earlier data obtained with various DNA samples (*10*, *29*, *30*). At more negative potentials, where reorientation and/or desorption of the DNA molecules may take place, striking differences were observed in the occurrence and intensity of the peaks in the four DNA samples studied.

Nicked DNA (open circular) displays the largest ΔC and the highest peak 1 (−1.19 V) (Table 1, Figure 1D). A high peak 3 (at −1.43 V) is observed, in contrast to the other three DNA samples (Figure 1A−C). Peaks 1 and 3 were also observed earlier with linear DNA of different sequence (*10*). Peak 1 was attributed to reorientation of the DNA molecule at the surface. Peak 3 is characteristic of denatured DNA and was aligned to segmental desorption of DNA attached to the surface via bases. In the measurements with the HMDE, the potential is scanned relatively slowly to more negative values over a range of more than 1 V. Thus the peaks obtained with the HMDE can be influenced by changes in the DNA structure that may occur at potentials less negative than the potential of the peak. It has been shown that appearance of peak 3 in linear dsDNA is connected with partial DNA unwinding at the electrode in a narrow potential range around −1.2 V (at neutral pH). The presence of peak 3 in nicked DNA suggests that this DNA, in common with linear DNA, undergoes unwinding at the electrode. This unwinding of nicked DNA requires accessibility of bases in the vicinity of the strand break for the interaction with the electrode (*10*, *31*−*33*).

Table 1: Values of Peak Heights and Capacitive Current Decrease Obtained with Rel, Scn, sch, and Oc PUC19 DNA[a]

DNA sample	(10^{-8} F)			
	p1	p3	p3*	ΔC
rel[b]	0.3		0	8.4
rel[c]	0.8		0	9.9
nsc[b]	1.4		0.2	10.9
hsc[b]	1.5		0.7	11.0
oc[b]	1.6	1.3		11.5

[a] p1, p3, and p3* are heights of peaks 1, 3, and 3*, respectively. ΔC is differential capacity decrease measured at −0.35 V vs SCE. [b] 100 μg mL^{-1}, t_A = 120 s. [c] 250 μg mL^{-1}, t_A = 180 s; for other conditions, see Figure 1.

With the dropping mercury electrode, the mercury surface is frequently renewed (usually in 1−10 s), and a new measurement is performed on each mercury drop; thus the AC impedance peaks cannot be influenced by any changes in DNA structure that occur at potentials differing from the peak potential. Peak 3 is thus not observed with linear (not shown) and open circular DNA (Figure 2) if a dropping mercury electrode is used in place of HMDE, in agreement with the nature of the unwinding process responsible for this peak. Unwinding of the double-stranded nicked DNA is negligible in this experiment, while single-stranded DNA produces a high peak 3 under the same conditions (Figure 2).

Covalently closed circular duplex DNA relaxed by topoisomerase I produces peaks 1 and 3, which are substantially smaller than those of nicked DNA using the HMDE (Figure 1B,D; Table 1). Peak 3 is probably due to a small amount of nicked DNA contaminating the sample of relaxed DNA, as it (in common with nicked DNA) strongly increases after exposure of the sample to denaturing conditions (not shown). The capacitance change of relaxed DNA (using the HMDE) corresponds to about 58% of that of nicked DNA, but the peak 1 height of relaxed DNA corresponds only to 17% of peak 1 of nicked DNA.

Highly negatively supercoiled DNA produces a new peak 3* at E_p= −1.38 V (Figure 1C), which is about 50 mV more positive than peak 3 from open circular DNA. If a small amount of open circular or denatured DNA is added to highly supercoiled DNA, both peaks can be observed, well separated

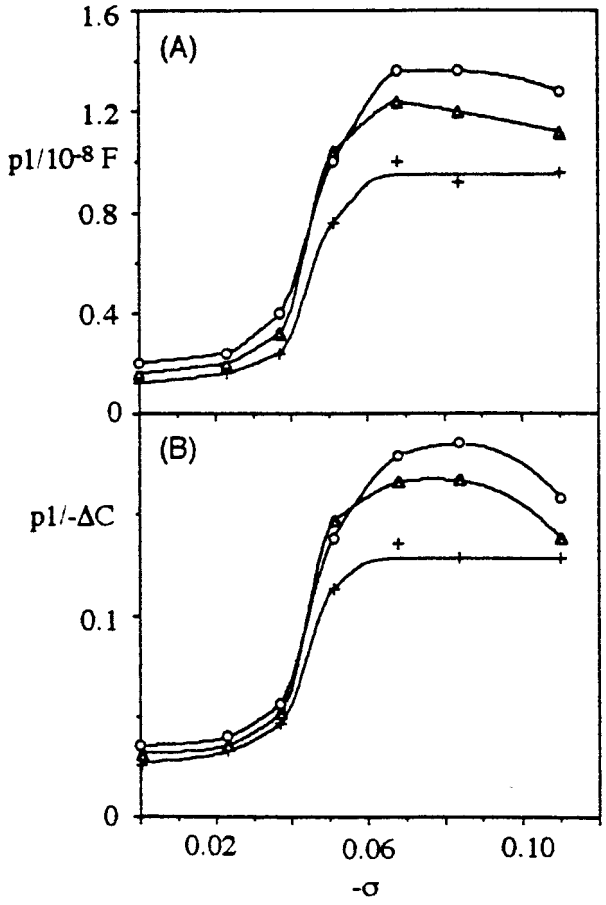

FIGURE 3: Dependence of height of peak 1 (p1) (A) and the ratio of p1 to the decrease of differential capacitance (ΔC) at −0.35 V (p1/ΔC) (B) for covalently closed circular pColIRΔXba DNA on its superhelix density. DNA at concentrations of 40 (+), 60 (△), and 80 (○) μg mL^{-1} was adsorbed from NT buffer for $t_A = 120$ s. Measurements were performed in 0.3 M NaCl and 0.03 M $NaHCO_3$, pH 9.5. For other details see Figure 1.

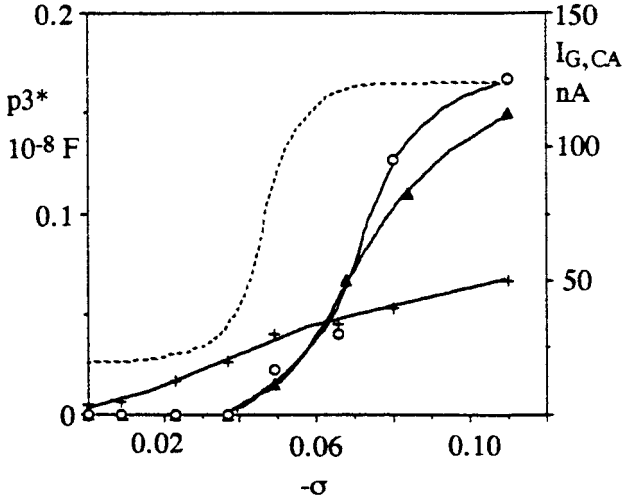

FIGURE 4: Dependence of the height of the AC *Z* peak 3* (▲) and cyclic voltammetric (CV) (redox) DNA peaks CA (due to reduction of cytosine and adenine, ○) and G (due to guanine, +) of covalently closed circular pColIRΔXba DNA on superhelix density. For measurements of peaks CA and G, 0.3 M ammonium formate 50 mM sodium phosphate, pH 6.9, was used as a background electrolyte. For other details see Figure 1.

from each other (not shown). Thus, peak 3* is not connected to peak 3. The height of peak 1 and the corresponding value of ΔC are slightly lower than those of supercoiled DNA at native superhelix density (nscDNA), which produces only a very small peak 3* (Figure 1A, Table 1). Nicking of relaxed, native, and highly supercoiled DNA in solution resulted in practically identical $C-E$ curves of open circular DNA. Relaxed, native, and highly supercoiled forms of other plasmid DNA (pAT153, pColIRΔXba, pUC19, and pBR322) produced qualitatively the same results (not shown).

First Structural Transition at $-\sigma \sim 0.04$. Our measurements reveal differences in the adsorption behavior of relaxed, native, and highly supercoiled DNA (Figure 1). We were interested whether the observed changes are a monotonic function of $-\sigma$ or whether they show an abrupt change that may correspond to some transition in the DNA structure. We therefore prepared topoisomer distributions of different mean superhelix density by means of relaxation by topoisomerase I in the presence of different concentrations of the intercalator ethidium bromide.

We measured $C-E$ curves for a set of topoisomer distributions of pAT153 and pColIRΔXba with mean superhelix density of $-\sigma = 0.009$, 0.023, 0.037, 0.049, 0.067, 0.081, and ≥ 0.11. Figure 3 shows a S-shaped dependence of peak 1 height (p1) on $-\sigma$ obtained for pColIRΔXba at DNA concentrations of 40 and 80 μg mL^{-1}. Within this range there are two regions of superhelix density in which the peak 1 height varied only slightly with superhelix density: the region from $-\sigma = 0$ to about 0.03 and that from $-\sigma \geq 0.06$. Between these two regions a sharp increase of peak 1 height was observed (transition TI), with a midpoint at about $-\sigma = 0.044$, which was almost independent of the DNA concentration over the range studied (Figure 3A). In principle, the increase in peak 1 height could be due to either an increase in the DNA surface concentration or changes in the ability of the DNA to respond to the alternating voltage (in the potential range where DNA segmental desorption or reorientation is taking place). At partly covered surfaces, changes in the DNA diffusion coefficient may result in changes in the peak height. Since ΔC at −0.35 V increases with the DNA surface concentration, but is not connected with the DNA desorption/reorientation processes, calculation of p1/ΔC removes the influence of DNA surface concentration on the peak 1 height. Plots of p1/ΔC show similar transitions to those seen in Figure 3A. This suggests that, although the observed dependence of peak 1 height on $-\sigma$ (Figure 3B) is influenced by changes in the DNA surface concentrations of different topoisomers, the observed sharp transition is due to changes in DNA features that influence its ability to respond to the alternating voltage.

Second Transition at $-\sigma = 0.07$. Peak 3* (Figure 1C) was not observed in the study of topoisomers of low superhelix density, but appeared at a superhelix density of about $-\sigma = 0.05$ as a very small signal. This was also observed in studies of pUC19 DNA (Figure 1A) and pColIRΔXba at native superhelix density. At more negative σ the height of peak 3* (p3*) increased, displaying an S-shaped dependence (Figure 4) with a midpoint at about $-\sigma = 0.07$ (transition TII). Peak 3* most probably arises from the desorption of the DNA segments with single-stranded character whose bases, in contrast to those of denatured DNA, cannot freely adhere to the electrode surface

due to topological restraint. This is supported by the close proximity of potentials of peak 3* and peak 3 (the latter peak is produced by denatured DNA or partially unwound DNA with free ends) and by analogy with the differential pulse polarographic (reduction) peak III (produced by denatured DNA) and less negative peak II (characteristic for distortions in the DNA) (*10*, *14*) separated by about 50−70 mV. If peak 3* reflects an increase in accessibility of bases, this should also be detectable by other methods. We used two approaches, based on the single-strand-selective chemical probe Os,bipy and on electrochemical reduction and oxidation signals produced at neutral pH.

Chemical Probing. Pyrimidine (preferentially thymine) bases may react with osmium tetroxide in the presence of bipyridine to form an adduct at the 5,6 bond. However, attack is inefficient when the base is present in normal duplex DNA, and elevated reactivity indicates structural distortion of the DNA that leads to exposure of the edge of the base. We treated relaxed, linear, native, and highly supercoiled pBR322 and pAT153 DNA with 2 mM Os,bipy for 30 min at 26 °C. The degree of modification of the DNA samples was determined in four ways: (a) by cleavage of the modified and control DNA samples with S1 nuclease, following linearization with *Bam*HI, (b) by immuno dot blotting using a monoclonal anti-DNA-Os,bipy antibody, (c) by UV spectrophotometry, and (d) by differential pulse stripping voltammetry, which makes it possible to determine the electroactive DNA−Os,bipy adduct (*34*, *35*).

S1 Nuclease Cleavage. Relaxed, linear, native, and highly supercoiled pAT153 were modified with 2 mM Os,bipy and subsequently linearized with *Bam*HI. The samples were then treated with S1 nuclease to cleave the DNA at positions rendered single-stranded due to adduct formation. Virtually no cleavage was observed using linear and relaxed DNA, while native supercoiled DNA lead to a smear and three weak bands corresponding to fragments of about 2700, 2300, and 1700 bp (Figure 5). With Os,bipy-modified highly supercoiled DNA, strong S1 nuclease cleavage was observed resulting in a smear and a set of narrower bands corresponding to fragments of about 3400, 2700, 2300, 1700, and 1200 bp (Figure 5). A quantitative estimation of the DNA distribution was made from the band intensities measured by densitometric tracing. In the case of relaxed and linear DNA, almost 100% of DNA was detected in the bands corresponding to full-length DNA molecule. With native and highly supercoiled DNA, 16 and 58% of DNA molecules, respectively, were cleaved into fragments.

Differential Pulse Stripping Voltammetry. DNA modified by Os,bipy (DNA−Os,bipy) produces several voltammetric signals due to osmium reduction (*36*, *37*). The most negative of them (at about −1.1 V) was shown to be suitable for a highly sensitive determination of DNA−Os,bipy (*35*). Using denatured DNA fully modified with Os,bipy for calibration, we used this peak to determine the extent of modification of various plasmid forms. In highly supercoiled DNA, the content of modified pyrimidine bases was calculated to be about 3.3%. Since Os,bipy modification of cytosine requires longer reaction times than thymine (*26*), all of these modified bases are likely to be thymines. Thus, up to 6% of thymine residues in highly supercoiled DNA may be modified. With nscDNA, smaller signal suggesting modification of less than 1% pyrimidines was observed (Table 2, Figure 6). With

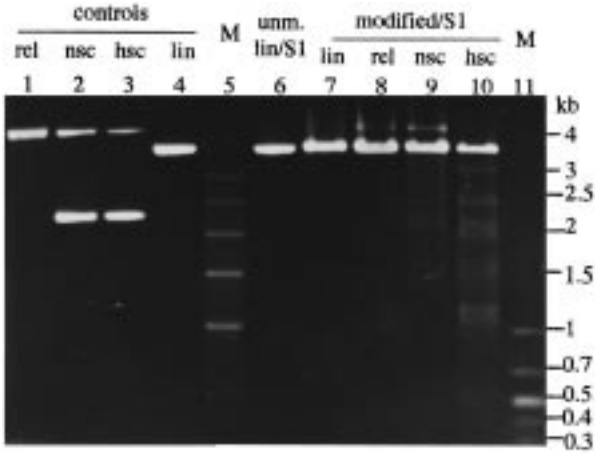

FIGURE 5: Agarose gel electrophoresis of pAT153 DNA modified with 2 mM Os,bipy after cleavage by S1 nuclease. Tracks 1−4, untreated controls (0.5 μg of DNA per track); 5 and 11, size markers (fragment lengths indicated at right); 6, unmodified and S1 nuclease-cleaved; 7−10, modified and S1-cleaved; 1 and 8, relaxed DNA; 2 and 9, native supercoiled DNA; 3 and 10, highly supercoiled DNA; 4 and 6, linear DNA. 2.5 μg of the DNA samples were modified with 2 mM Os,bipy in SSC buffer at 21 °C for 25 min and subsequently linearized with *Bam*HI. The linearized DNA was cleaved with 0.15 U mL^{-1} S1 nuclease for 30 min at 37 °C and loaded on the gel.

Table 2: Reactivity of Various Forms of pAT153 DNA toward Os,Bipy[a]

sample	modified pyrimidines (%)
den[b]	100
den[c]	28
hsc[c]	3.3
nsc[c]	0.6
rel[c]	0[d]
lin[c]	0[d]

[a] The Os,bipy modified pyrimidine residues were determined by differential pulse voltammetry. [b] DNA modified with 4 mM Os,bipy at 37 °C for 20 h. [c] DNA modified with 2 mM Os,bipy at 26 °C for 30 min. [d] Below the detection limit. For more details, see Figure 6.

relaxed and linear DNA, no signal around −1.1 V corresponding to the adduct was observed.

Spectroscopic measurements based on an adduct-specific band around 310 nm (*26*) yielded quantitatively similar data (suggesting about 2.9% modified pyrimidines in hscDNA).

Immuno dot blotting analysis using the anti-DNA−Os,bipy monoclonal antibody OsBP95-1 (*27*) revealed significant Os,bipy modification in highly supercoiled pAT153 (the estimated signal intensity was <1% measured against serial dilutions of fully modified denatured DNA) and a very weak signal of modified native supercoiled DNA. The extent of Os,bipy modification in other DNA samples was below the limit of detection of the method under the given conditions.

Voltammetric Redox Peaks. At neutral and acid pH, cytosine and adenine residues in ssDNA are reduced at the mercury electrode, generating a voltammetric peak called CA at about −1.4 V. Guanine residues are reduced at highly negative potentials (around −1.8 V), and the guanine reduction product is oxidized back to guanine producing an anodic peak called G in cyclic voltammetric modes. The primary reduction sites of C and A are hidden in the interior of the DNA double helix participating in Watson−Crick

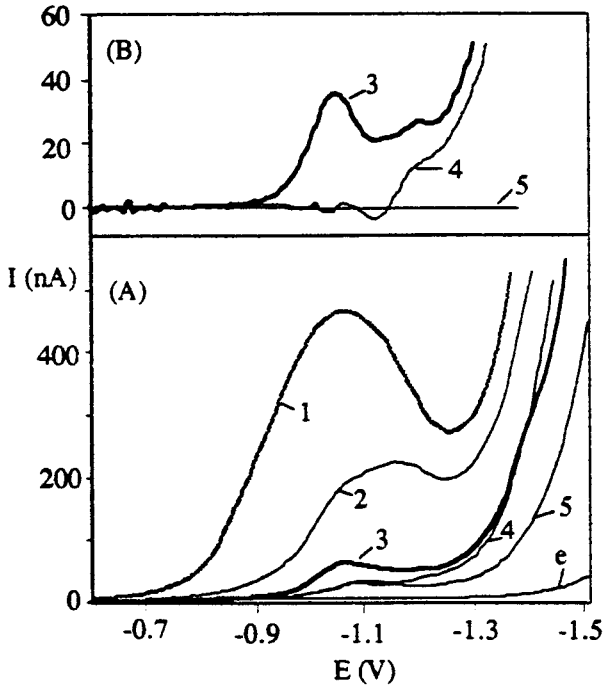

FIGURE 6: AdTS differential pulse voltammograms of pAT153 (2 μg/sample) modified with Os,bipy in SSC buffer. 1−2, denDNA; 3, hscDNA; 4, linDNA; 5, control (DNA-free); e, background electrolyte; 1, 4 mM Os,bipy, 20 h, 37 °C; 2−5, 2 mM Os,bipy, 30 min, 26 °C; A, the raw voltammograms; B, curves obtained after the control curve (5) subtraction. After the modification and ethanol precipitation, DNA (dissolved in 20 μL) was nicked with DNase I, followed by thermal denaturation. After the addition of NT buffer DNA was adsorbed at the electrode for 2 min. For other details see Methods.

hydrogen bonding. The reduction site of guanine is the double bond between N7−C8 located in the major groove. Accordingly peak CA is more sensitive to changes in the DNA structure than peak G (*12*).

We used cyclic voltammetry (CV) to measure the dependence of the heights of peaks CA (I_{CA}) and G (I_G) of pColIRΔXba on superhelix density. As shown in Figure 4, the dependence of I_{CA} is very similar to that of p3* obtained under similar conditions: no peak CA appeared with topoisomers of $-\sigma < 0.04$, and a S-shaped dependence of I_{CA} was observed at higher negative superhelix densities, with a transition point at $-\sigma$ about 0.07. On the other hand, I_G increased monotonically with $-\sigma$ revealing no transition in the range of superhelix density employed (Figure 4). These results suggest that the changes in the DNA structure responsible for the observed transition TII are more subtle than those resulting from thermal denaturation or from various kinds of the damage to double-stranded DNA, which are reflected both by changes in I_{CA} and (though less sensitively) in I_G.

Calculating the amount of accessible bases in scDNA from the heights of peak CA is difficult because of lack of an appropriate standard for supercoiled DNAs. Relative comparison of I_{CA} of native and highly supercoiled DNA suggests that highly supercoiled DNA exposes 3.7 times more bases as compared to native supercoiled DNA. This number is in a reasonable agreement with the results of voltammetric determination of Os,bipy binding to these DNA species.

The above results suggest that in highly supercoiled DNA a substantially larger amount of bases is available for the interaction with the environment as compared to native supercoiled DNA and topoisomeric samples with less negative superhelix density. In the latter samples the amount of accessible bases was below the detection limit of the immuno dot blotting and electrochemical determination of the DNA−Os,bipy adducts.

DISCUSSION

DNA topology is intimately linked to both local and global conformation in closed circular DNA. Significant progress has been made in the understanding of the conformational properties of supercoiled DNA in recent years, both in experimental and theoretical terms (*6*, *38*−*41*). Small DNA circles (<300 bp) undergo a global structural transition from a flat structure to a figure-8 conformation at a certain critical linking difference (ΔLk) (*5*, *6*, *41*−*46*). Sharp changes in writhe (Wr) of a 178 bp DNA circle as a result of increased concentration of counterions at $\Delta Lk = -2$ were observed by electron microscopy (*5*). Olson and Schlick (*43*) predicted another sharp conformational transition at higher levels of supercoiling, involving discontinuous changes of Wr with ΔLk for short DNA molecules. These transitions should not be expected in long DNA molecules however (such as the plasmids used in this study) where Wr/ΔLk is independent of superhelix density (*6*).

Our AC impedance measurements showed that various forms of circular plasmid DNA adsorb at the electrically charged mercury/water interface in a wide potential range, similar to previously studied native double-stranded and denatured chromosomal DNA (reviewed in ref *10*). A detailed comparison of the C−E curves of relaxed, native, and highly supercoiled DNA revealed quantitative differences in ΔC and in the height of peak 1 (Figures 1 and 3), suggesting that these DNA species may interact with the electrically charged surface and respond to the alternating voltage in different ways. Qualitative differences were observed at highly negative potentials where highly supercoiled DNA gave rise to peak 3* (Figure 1C), which had not previously been observed. Analysis of topoisomeric samples with superhelix densities ranging from $-\sigma = 0$ to 0.11 revealed S-shaped dependences of ΔC and heights of peaks 1 and 3* on $-\sigma$ (Figures 3 and 4) suggesting the occurrence of two transitions. What is the nature of these transitions?

For covalently closed circular plasmid DNA, translational diffusion coefficients depend on superhelix density because the shape of the DNA molecule is dependent on superhelix density (*47*). Differences in the diffusion rates of the topoisomers might affect the surface concentration of DNA at partially covered surfaces. Previous studies of chromosomal DNA and polynucleotides (*10*, *48*) suggested that diffusion was a rate-limiting step in the adsorption of linear nucleic acid at partially covered surfaces. If the same is true for the covalently closed circular DNA, the increase in ΔC and the heights of peaks 1 and 3* might be due to greater rate of transport of the DNA molecules with higher linking differences under the conditions of partially covered surfaces. However, this is unlikely because earlier it was shown (*49*−*51*) that the sedimentation coefficient of bacteriophage PM2 DNA (10 kb) rises to a maximum at $-\sigma = 0.05$ and then decreases to its minimum close to $-\sigma = 0.1$. Translation

diffusion coefficients measured by dynamic light scattering coupled with computation (*47*) increased monotonically as a function of linking difference and reached a limiting value at high ΔLk. Thus, the observed transitions TI and TII and the differences in $C-E$ curves of different plasmid forms are not caused by altered diffusion coefficients.

Changes in Responses to Alternating Voltage of Adsorbed DNA at Moderate Superhelix Density. Superhelix density-dependent properties of large supercoiled DNA species (2687−7238 bp) were calculated from the fluorescence anisotropy of intercalated ethidium, circular dichroism, dynamic light scattering, and other techniques (*45*, *52*, *53*). Song et al. (*53*) observed two transitions at midpoint superhelix densities $-\sigma = 0.020$ and 0.035, which they explained as superhelical stress-induced structural transitions in global DNA secondary structure. The transition at $-\sigma = 0.035$, detected by measuring the torsion constant of the pUC8 dimer, is shifted only by about 0.009 to less negative σ values as compared to the transition TI described in this paper (Figure 3). Considering the differences in the sizes of the plasmid DNA, the conditions, and the nature of the DNA properties monitored, it seems probable that the transitions close to $-\sigma = 0.04$ observed by Song et al. (*53*) and by us (Figure 3) may reflect different aspects of the same superhelix-dependent changes in DNA structure. While the results obtained by Song et al. were explained in terms of altered secondary structure, changes in the DNA adsorbability observed here (Figures 1−3) may depend on the ability of the DNA to respond to the alternating voltage. Such changes may be connected with different ways of attaching the DNA to the surface and/or with an alteration in flexibility of the DNA segments. The flexibility of the DNA is likely to be related to internal motions within the DNA molecules, and it is notable that Langowski et al. (*45*) observed an increase in the pUC18 DNA internal diffusion coefficient starting from $-\sigma = 0.03$ and a maximum of the internal motion amplitude near the same σ value. Positioning of the DNA molecule at the surface of the electrode might also be influenced by the shape of the DNA molecule. Thus, sudden changes in branching of the interwound DNA or a transition from the interwound form to the toroidal one might result in an abrupt change in the DNA adsorption behavior. This behavior could be also modified by changes in the DNA secondary structure, as it has been shown (*14*) that DNA melting and premelting is reflected by changes in the adsorption of DNA at the mercury electrode. At this stage our data do not allow us to decide whether the changes in the DNA tertiary structure and the global shape of the DNA molecule or the changes in the DNA secondary structure are responsible for the transition TI (Figure 3). Due to the similarity of the transition TI and the transition observed by Song et al. (*53*), it seems probable that changes in DNA secondary structure are involved in transition TI.

Base Pair Opening at Highly Negative Superhelix Density. The transition with a midpoint at $-\sigma = 0.07$ monitored by changes in the height of peak 3* (Figure 4) is clearly connected with opening of the DNA duplex, making some bases more available for interaction with the environment. This assumption is supported by the results of the chemical probing (Figure 5) and changes in the voltammetric reduction peak CA (Figure 4). The presence of peak 3* in the curve of highly supercoiled DNA (Figure 1C) suggests that an appreciable fraction of this DNA tends to desorb from the surface at less negative potentials as compared to denatured and nicked DNA. The latter DNA contain hydrophobic bases freely accessible for the interaction with the hydrophobic surface of the mercury electrode. The total extent of helix opening in covalently closed circular DNA is topologically limited, and the accessible bases in highly supercoiled DNA are contained mainly in short nucleotide stretches (see below) resulting in a less firm adsorption as compared to denatured DNA and easier segmental desorption in a less negative peak 3*.

Brahms et al. (*54*) studied the effect of the superhelix density of a set of negatively and positively supercoiled plasmids on their circular dichroism (CD) and Raman spectra. They observed a linear increase of the positive CD bands (at 262, 278, and 290 nm) with increasing $-\sigma$ from 0 to 0.07. At a superhelix density higher than $-\sigma = 0.07$, the change in the slope reflected a transition to a new conformation with different spectral features. This transition was explained by formation of left-handed DNA at high negative superhelix density. The midpoint of the transition TII observed in this paper by measuring the height of peak 3* (Figure 1C) agrees well with the results of Brahms et al. (*54*). However, our results cannot be explained exclusively by formation of left-handed DNA. Using the single-strand selective reagent Os,bipy, we calculate from the voltammetric and spectroscopic adduct determination that in highly supercoiled DNA ($-\sigma = 0.11$) about 3.3% of pyrimidine bases are accessible to the probe (Figure 6). Our dot blotting analysis qualitatively agrees with the results of the electrochemical analysis, although quantitative evaluation of the immunochemical data was not possible because of lack of an adequate calibration. The monoclonal anti-DNA−Os,bipy antibody OsbBP95-1 (*27*) is highly sensitive for long stretches of Os,bipy-modified nucleotides in DNA, but it is incapable of detecting short nucleotide stretches and isolated nucleotides. If the fully modified, thermally denatured DNA were taken as a standard, then the immunoassay would give an estimate for the amount of reactive bases that is about 4 times lower than the electrochemical determination. Comparing these two determinations, we may conclude that the majority of the reacted bases are contained in short stretches or in isolated nucleotides not recognized by the antibody. Increased reactivity of DNA toward the Os,bipy need not be restricted to unpairing of bases, but in addition it could arise from various distortions of the double helix including base unstacking or changes in twist.

The question of formation of DNA noncanonical structures in naturally occurring sequences of supercoiled DNAs was studied both experimentally (*1*, *55*, *56*) and theoretically (*57*−*59*). Statistical mechanical models were developed capable to predict formation of Z-DNA and cruciform structures in various DNAs. The increased chemical reactivity of Z-DNA in $d(CA/TG)_n$ sequences was explained by theoretically predicted distribution of the junctions between B- and Z-DNAs (*59*). Probing of the $d(AC/GT)_{32}$ sequence in a supercoiled pRW777 DNA at $-\sigma = 0.091$ showed that the extent of modification was below 50%, even at $-\sigma = 0.112$ (*55*). If all thymines contained in 10 sequences with the highest Z-DNA forming potential in pBR322 (*58*) were fully modified under our experimental conditions, the amount of modified thymines would correspond to about 1% of all

pyrimidines in pBR322. However, a more realistic estimate would be much lower. Thus, 3.3% of pyrimidine bases accessible to Os,bipy cannot be explained by hyperreactivity of Z-DNA segments.

It is possible that, at highly negative superhelix densities, other local structures such as cruciforms and triplexes as well as base unpaired regions may be formed in sequences of imperfect inverted repeats, homopurine·homopyrimidine, and A+T-rich stretches, respectively. The above local structures may contain many structural imperfections (such as looped out and mismatched bases) providing further Os,bipy-reactive bases in addition to cruciform and triplex loops, and B−Z junctions. The increased smear observed on the gel with the highly supercoiled DNA (Figure 5) suggests that a portion of bases is modified at random probably due to increased DNA "breathing".

The recent twin supercoiled domain model for transcription suggests that positive supercoils may be formed downstream and negative supercoils may be formed upstream from translocating RNA polymerase (*60*, *61*). In this manner high local levels of negative supercoiling might be created behind the transcription complex under some circumstances. The base pair opening at highly negative superhelix density described in this paper may thus have some biological relevance.

ACKNOWLEDGMENT

The authors are indebted to Professor Maxim Frank-Kamentskii for critical reading of the manuscript.

REFERENCES

1. Paleček, E. (1991) *Crit. Rev. Biochem. Mol. Biol. 26*, 151−226.
2. Bowater, R., Aboul-ela, F., and Lilley, D. M. J. (1992) in *Methods in Enzymology* (Lilley, D. M. J., and Dahlberg, J. E., Eds.) pp 105−120, Academic Press, Inc., London.
3. Paleček, E. (1994) in *Nucleic Acids and Molecular Biology* (Eckstein, F., and Lilley, D. M. J., Eds.) pp 1−13, Springer-Verlag, Berlin.
4. Adrian, M., Heggeler-Bordier, B., Wahli, W., Stasiak, A. Z., Stasiak, A., and Dubochet, J. (1990) *EMBO J. 9*, 4551−4554.
5. Bednar, J., Furrer, P., Stasiak, A., Dubochet, J., Engelman, E. H., and Bates, A. D. (1994) *J. Mol. Biol. 235*, 825−847.
6. Vologodskii, A. V., and Cozzarelli, N. R. (1994) *Annu. Rev. Biophys. Biomol. Struct. 23*, 609−643.
7. Andrade, J. D., and Hladky, V. (1986) *Adv. Polym. Sci. 79*, 1.
8. Haynes, C. A., and Norde, W. (1994) *J. Colloids Surf. B 2*, 517.
9. Ramsden, J. J. (1993) *Q. Rev. Biophys. 27*, 41.
10. Paleček, E. (1983) in *Topics in Bioelectrochemistry and Bioenergetics* (Milazzo, G., Ed.) pp 65−155, John Wiley, London.
11. Paleček, E. (1986) *Bioelectrochem. Bioenerg. 15*, 275−295.
12. Paleček, E. (1996) *Electroanalysis 8*, 7.
13. Fojta, M., Vetterl, V., Tomschik, M., Jelen, F., Nielsen, P., Wang, J., and Paleček, E. (1997) *Biophys. J. 72*, 2285−2293.
14. Paleček, E. (1976) in *Progress in Nucleic Acid Research and Molecular Biology* (Cohn, W. E., Ed.) pp 151−213, Academic Press, New York.
15. Twigg, A. J., and Sherratt, D. (1980) *Nature 283*, 216−218.
16. Sambrook, J., Frisch, E. F., and Maniatis, T. (1989) *Molecular Cloning*, 2nd ed., Cold Spring Harbor Laboratory Press, New York.
17. Sullivan, K. M., and Lilley, D. M. J. (1986) *Cell 47*, 817−827.
18. Lilley, D. M. J. (1985) *Nucleic Acids Res. 13*, 1443−1465.
19. Singleton, C. K., and Wells, R. D. (1982) *Anal. Biochem. 122*, 253−257.
20. Pospíšil, L. (1996) in *Experimental techniques in biochemistry* (Brabec, V., Walz, D., and Millazo, G., Eds.) pp 1−39, Birkhauser Verlag, Basel.
21. Paleček, E., Jelen, F., Teijeiro, C., Fučík, V., and Jovin, T. M. (1993) *Anal. Chim. Acta 273*, 175−186.
22. Paleček, E., and Postbieglová, I. (1986) *J. Electroanal. Chem. 214*, 359−371.
23. Paleček, E. (1988) *Bioelectrochem. Bioenerg. 20*, 171−194.
24. Breyer, B., and Bauer, H. H. (1963) *Alternating current polarography and tensammetry*, John Wiley & Sons, New York.
25. Jehring, H. (1974) *Elektrosorptionsanalyse mt der Wechselstrom-Polarographie*, Akademie-Verlag, Berlin.
26. Jelen, F., Karlovský, P., Pečinka, P., Makaturová, E., and Paleček, E. (1991) *Gen. Physiol. Biophys. 10*, 461−473.
27. Kuderová, A., Pexa, T., Staňková, V., Lauerová, L., Kovařík, J., and Paleček, E. (1997) manuscript in preparation.
28. Teijeiro, C., Nejedlý, K., and Paleček, E. (1993) *J. Biomol. Struct. Dyn. 11*, 313−331.
29. Fojta, M., and Paleček, E. (1997) *Anal. Chim. Acta 342*, 1−12.
30. Brabec, V., and Paleček, E. (1972) *Biopolymers 11*, 2577−2589.
31. Paleček, E. (1992) *Bioelectrochem. Bioenerg. 28*, 71−83.
32. Brabec, V., and Paleček, E. (1976) *Stud. Biophys. 60*, 105−110.
33. Brabec, V., and Paleček, E. (1976) *Biophys. Chem. 4*, 79−92.
34. Paleček, E. (1992) in *Methods in Enzymology* (Lilley, D. M. J., and Dahlberg, J. E., Eds.) pp 139−155, Academic Press, London.
35. Paleček, E., and Hung, M. A. (1983) *Anal. Biochem. 132*, 236−242.
36. Lukášová, E., Jelen, F., and Paleček, E. (1982) *Gen. Physiol. Biophys. 1*, 53−70.
37. Lukášová, E., Vojtíšková, M., Jelen, F., Sticzay, T., and Paleček, E. (1984) *Gen. Physiol. Biophys. 3*, 175−191.
38. Rybenkov, V. V., Vologodskii, A. V., and Cozzarelli, N. R. (1997) *J. Mol. Biol. 267*, 312−323.
39. Rybenkov, V. V., Vologodskii, A. V., and Cozzarelli, N. R. (1997) *J. Mol. Biol. 267*, 299−311.
40. Rybenkov, V. V., Vologodskii, A. V., and Cozzarelli, N. R. (1997) *Nucleic Acids Res. 25*, 1412−1418.
41. Schlick, T. (1995) *Curr. Opin. Struct. Biol. 5*, 245−262.
42. Schlick, T., Li, B., and Olson, W. K. (1994) *Biophys. J. 67*, 2146−2166.
43. Schlick, T., Olson, W. K., Westcott, T., and Greenberg, J. P. (1994) *Biopolymers 34*.
44. Chirico, G., and Langowski, J. (1994) *Biopolymers 34*, 415−433.
45. Langowski, J., Kapp, U., Klenin, K., and Vologodski, A. (1994) *Biopolymers 34*, 639−646.
46. LeBret, M. (1979) *Biopolymers 18*, 1709−1725.
47. Langowski, J., Kremer, W., and Kapp, U. (1992) in *Methods in Enzymology, Vol. 211* (Lilley, D. M. J., and Dahlberg, J. E., Eds.) Academic Press, Inc., London.
48. Brabec, V., and Paleček, E. (1973) *Z. Naturforsch. 28C*, 685−692.
49. Upholt, W. B., Gray, H. B. J., and Vinograd, J. (1971) *J. Mol. Biol. 62*, 21−38.
50. Wang, J. C. (1969) *J. Mol. Biol 43*, 24−39.
51. Wang, J. C. (1974) *J. Mol. Biol 87*, 797−816.
52. Shibata, J. H., Wilcoxon, J., Schurr, J. M., and Knauf, V. (1984) *Biochemistry 23*, 1188−1194.
53. Song, L., Fujimoto, B. S., Wu, P., Thomas, J. C., Schibata, J. H., and Schurr, J. M. (1990) *J. Mol. Biol. 214*, 307−326.
54. Brahms, S., Nakasu, S., Kikuchi, A., and Brahms, J. G. (1989) *Eur. J. Biochem. 184*, 297−303.
55. Galazka, G., Paleček, E., Wells, R. D., and Klysik, J. (1986) *J. Biol. Chem. 261*, 7093−7098.

56. Kladde, M. P., Kohwi, Y., Kohwi-Shigematsu, T., and Gorski, J. (1994) *Proc. Natl. Acad. Sci. U.S.A. 91,* 1898−1902.
57. Anshelevich, V. V., Vologodskii, A. V., and Frank-Kamenetskii, M. D. (1988) *J. Biomol. Struct. Dyn. 6*, 247−259.
58. Ho, P. S., Ellison, M. J., Quigley, G. J., and Rich, A. (1986) *EMBO J. 5*, 2737−2744.
59. Ho, P. S. (1994) *Proc. Natl. Acad. Sci. U.S.A. 91*, 9549−9553.
60. Liu, L. F., and Wang, J. C. (1987) *Proc. Natl. Acad. Sci. U.S.A. 84*, 7024−7027.
61. Wu, H. Y., Shyy, S. H., Wang, J. C., and Liu, L. F. (1988) *Cell 53*, 433−440.

BI9729559